Digest Journal of Nanomaterials and Biostructures Vol. 5, No 2, July-September 2010, p. 623 – 628

ANIONIC, CATIONIC AND NONIONIC SURFACTANTS-ASSISTED HYDROTHERMAL SYNTHESIS OF TIN OXIDE NANOPARTICLES AND THEIR PHOTOLUMINESCENCE PROPERTY

S. GNANAM*, AND V. RAJENDRAN
Department of Physics, Presidency College, Chennai-600 005, Tamilnadu, India.

Nanocrystalline tin oxide (SnO_2) powders of about 8-13nm in size have been successfully synthesized by using different surfactants such as cetyltrimethyl ammonium bromide (CTAB), sodium dodecyl sulphate (SDS), and poly ethylene glycol (PEG) via hydrothermal method. The products were characterized by means of powder X-ray diffraction (XRD), Scanning electron microscopy (SEM), Transmission electron microscopy (TEM), UV-absorption spectroscopy and Photoluminescence (PL) spectroscopy. The flower petals, florets of cauliflower, and sheet and rods like morphologies of the prepared SDS, CTAB, and PEG mediated SnO_2 were observed in the SEM micrographs. The photoluminescence emission band was at near 395nm and no other bands were observable, which proved to exhibit high optical property and might have potential application in nanoscale optoelectronic devices.

(Received May 5, 2010; accepted June 4, 2010)

Keywords: Semiconductor; Tin oxide; Nanoparticles; Hydrothermal process and Photoluminescence

1. Introduction

In recent years, nanosize semiconductor has been extensively investigated due to its special electrical and optical characteristics in fabricating nanoscaled electronic and optoelectronic devices. At present the growth, processing, and characterization of nanorods and nanoparticles is of global interest. There is an intensive research for controlling and manipulating nanostructured materials. This is of interest for both fundamental understanding as well as for potential technological and medical applications. Tin oxide (SnO_2), an n-type semiconductor with a wide band gap (Eg= 3.6 eV at 300 K), is extensively used as a functional material for optoelectronic devices [1], conductive electrodes and transparent coatings due to its good conductivity and transparency in the visible spectrum [2,3], solar cells [4,5], and catalyst support [6]. Nanostructured SnO_2 particles have been prepared by using different chemical methods such as precipitation, hydrothermal, sol-gel, gel-combustion and spray pyrolysis [7-14].

Among the above methods to prepare SnO_2, hydrothermal synthesis route, as an important method for wet chemistry, has been attracting material chemists' attention. The hydrothermal processing is an alternative to calcination for the crystallization of SnO_2 under mild temperature. However, it was still difficult to control the size of nanoparticles. Recently, it has been noted that anionic, cationic and nonionic surfactants can be used to assist the formation of nanoscaled materials.

The main purpose of the present research is to study the influence of cationic, anionic and nonionic surfactants on the size, morphology and hence, photoluminescence properties of the synthesized nanomaterials were investigated.

---

*Corresponding author: gnanam.sambatham@gmail.com

2. Experimental

In a typical synthesis, Firstly at 60°C, 1.68g anionic surfactant (SDS) was added to 80 ml of water until the pH reached 1.5 with magnetic stirring. Then, 16 ml of water and 18g of $SnCl_4.5H_2O$ were added and dissolved in above solution. Secondly, 10ml ethylene glycol were then added into the above solution and stirred for 20min to form a sol. Thirdly, 30ml aqueous ammonia solution was added drop wise to the above sol within 30min under magnetic stirring. Then the hydrolysis product was stirred for 30min to form a gel. Finally, the gel was transferred into a Teflon-lined autoclave for hydrothermal reaction at 160°C for 12h. After that, the black-brown hydrothermal product was filtered and dried at 120°C for 12h. The obtained black colored SnO_2 samples were calcinated at 400°C for 2h in order to eliminate the surfactant completely from the as- synthesized product. The same procedure was followed for the preparation of pale brown and pale greenish-brown SnO_2 nanoparticles using cationic (CTAB) and nonionic (PEG) surfactants.

The XRD pattern of the SnO_2 powder was recorded by using a powder X-ray diffractometer (Schimadzu model: XRD 6000 using CuKα (λ=0.154 nm) radiation, with a diffraction angle between 20 and 70°**.** The crystallite size was determined from the broadenings of corresponding X-ray spectral peaks by using Debye Scherrer's formula. Scanning Electron Microscopy (SEM) studies were carried out on JEOL, JSM- 67001. Transmission electron microscope (TEM) image was taken using an H-800 TEM (Hitachi, Japan) with an accelerating voltage of 100kV. UV-Vis absorption spectra for the samples recorded using a Varian Cary 5E spectrophotometer in the range of 200-800 nm for the powder samples (calcined at 400ºC) in nujol mode. The photoluminescence (PL) spectra of the SnO_2 were recorded by Perkin-Elmer lambda 900 spectrophotometer with a Xe lamp as the excitation light source.

3. Results and discussion

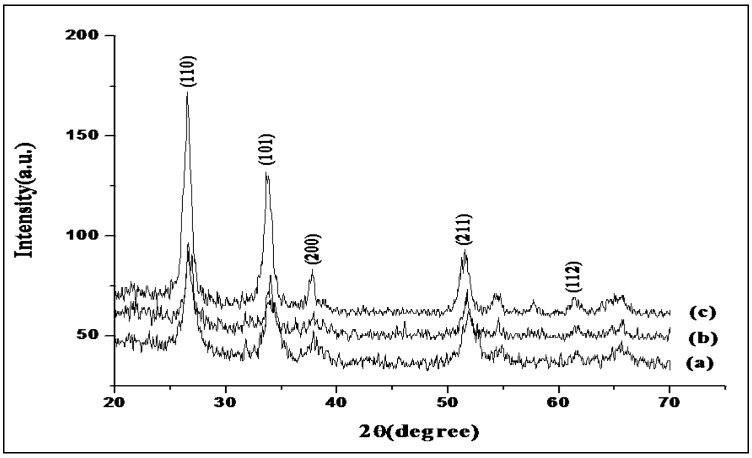

Fig.1. XRD patterns of tin oxide nanoparticles (a) SDS, (b) CTAB, and (c) PEG calcined at 400°C.

The XRD pattern of the as-obtained tin oxide nanoparticles is shown in Fig.1. All of the peaks in Fig.1a (SDS), 1b (CTAB) and 1c (PEG) can be well indexed to the tetragonal rutile structure of SnO_2 (JCPDS card no. 88-0287, a=4.737 Å and c=3.186 Å) with high crystallinity. No characteristic peaks of impurities, such as SDS, CTAB and PEG or other tin oxides were observed, indicating the high purity of the products. In Fig.1(c) (PEG), it is noted that the peak intensity of the samples was notably higher than that of the intensities in Fig.1 (a) (SDS) and 1(b) (CTAB) due to larger particle size. Using Debye Scherrer's formula, the crystallite sizes of SnO_2 nanoparticles can be determined. The average particle size, surface area and morphology of as-synthesized tin oxide nanoparticles are tabulated in table1.

Table1. The size, surface area and morphology of different surfactants assisted tin oxide nanoparticles.

Tin oxide samples	Particle size (D) nm	Surface area (m^2/g)	Morphology
SDS	8	112.10	Flower petal
CTAB	11	81.53	Florets of Cauliflower
PEG	13	68.98	Sheet and rods

The surface morphology of the samples obtained using SDS, CTAB and PEG as examined by SEM is shown in the Fig.2 (a-c). The SEM micrographs clearly show micro-structural homogeneities and remarkably different morphologies for SnO$_2$ prepared in different surfactants. Flower petal-like morphology was observed for the sample (a) (SDS) whereas the shape of the agglomerated particles of the sample (b) (CTAB) looked like the florets of cauliflower. In an aqueous system, CTAB ionize completely and result in cation with tetrahedral structure. The electrostatic interaction takes place between CTA$^+$ cations and Sn (OH) $_6^{2-}$ anions, the cation CTA$^+$ condense into aggregates in which counter ions Sn (OH) $_6^{2-}$ are interrelated in the interfaces between the head group to form CTA$^+$- Sn (OH) $_6^{2-}$ pair .The sheet- or rod-like morphology was observed for sample (c) (PEG). PEG being a non-ionic surfactant SnO$_2$ formation was not possible due to the electrostatic interaction and was due to weak Vander wall's interaction, and the acidic solution could provide protons binding to PEG molecules via hydrogen bonding [15]. The lower particle size and different morphology reveals the key role of individual surfactants in controlling the nucleation and crystal orientation.

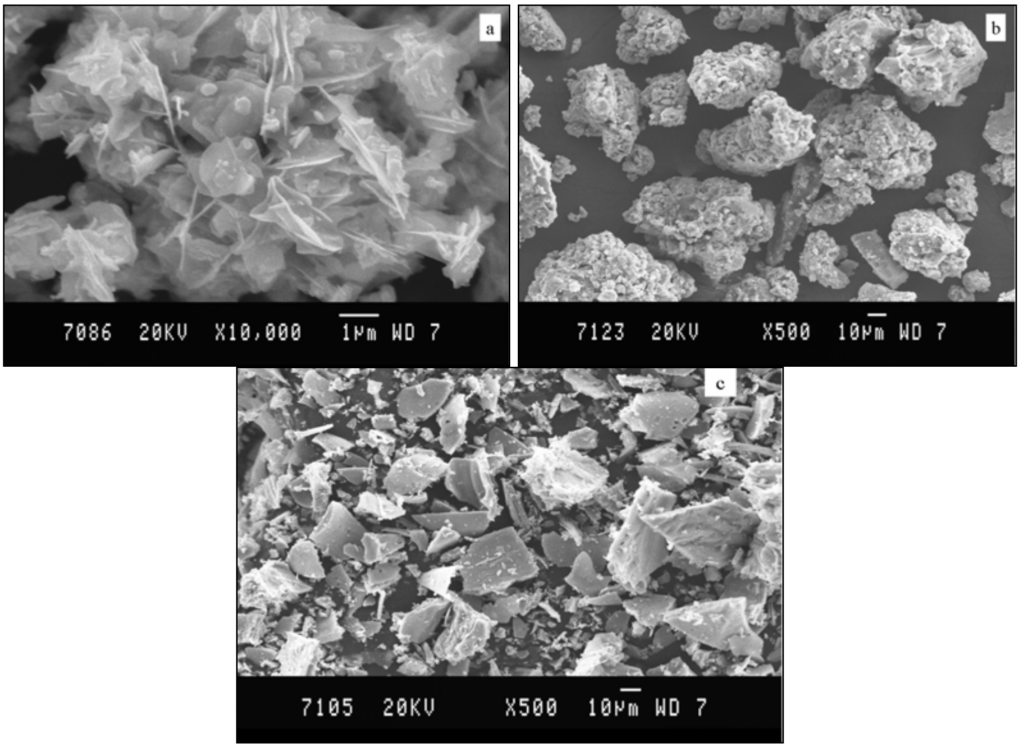

Fig.2 SEM images of tin oxide nanoparticles (a) SDS, (b) CTAB, and (c) PEG.

The TEM image of SDS assisted SnO_2 products were shown in Fig.3. It is noted that the product mainly consist of flake like, well-dispersed nanoparticles with an average particle size about 7 nm. Moreover, the particle size of the sample obtained from TEM pattern is comparable to those calculated from Scherrer's equation. In our studies the surfactants possibly acts as a soft template, we believe that the nanoparticles fabricated through our approach grow mainly by Oswald ripening mechanism. Initially many nanoparticles with different sizes appear in the solution with the reaction proceedings, the nanoparicles with the larger size grow at the cost of smaller ones due to higher surface free energy [16]. Particle formation is very complex process. It involves nucleation, growth, and coagulation, flocculation, all which may be influenced significantly by the surfactant assemblies. Therefore, SDS plays an important role in the preparation of tin oxides nanoparticles.

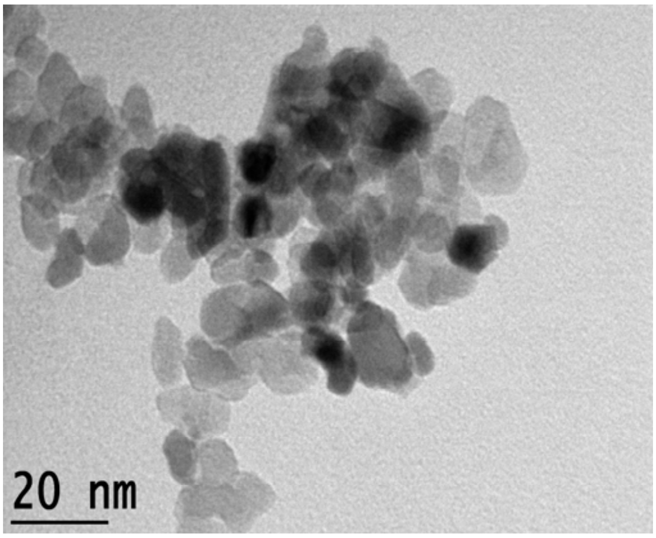

Fig. 3. TEM micrograph of the SDS-assisted tin oxide nanoparticles calcined at 400°C.

Fig.4 represents the UV absorption spectra of SnO_2 nanoparticles, and absorbance edges were observed at 312, 315, and 318nm for different surfactants mediated like SDS, CTAB, and PEG respectively (Fig.4a-c). In all the cases, blue shifts were observed.

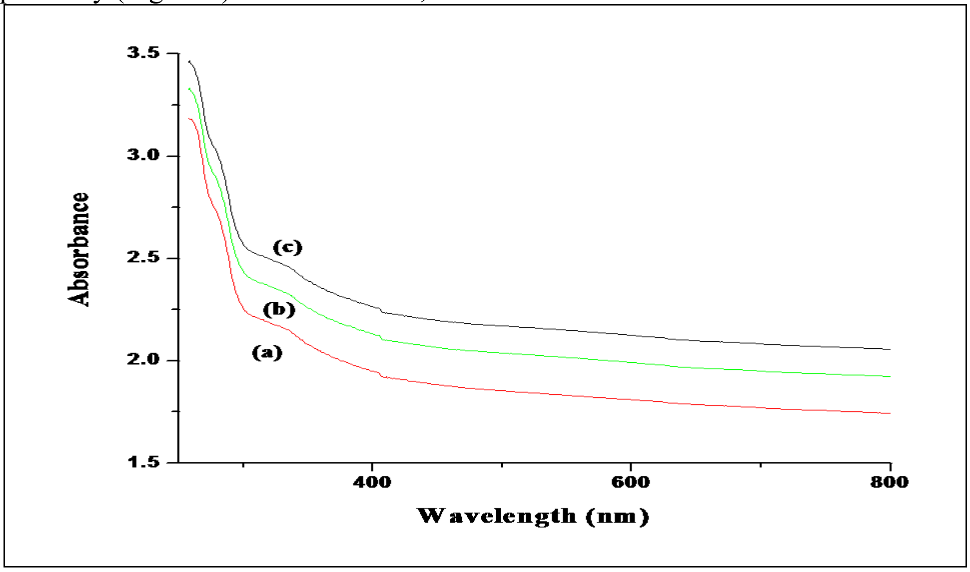

Fig.4. Absorption spectra of tin oxide nanoparticles (a) SDS, (b) CTAB, and (c) PEG.

Considering the blue shift of the absorption positions from the bulk SnO_2, the absorption onsets of the present samples can be assigned to the direct transition of electron in the SnO_2 nanocrystals. The corresponding band gap energies can be calculated to be 3.9eV, 3.93eV and 3.89eV and are larger than the bulk SnO_2 [17].

Fig.5 shows the room temperature PL spectra of the SnO_2 nanoparticles prepared from different surfactants, with an excitation wavelength of 325nm. The PL spectra have strong UV emission band peaking around 395nm. Particularly, SDS mediated tin oxide nanoparticles (Fig.5a) exhibited strong high intensity UV emission than that of the CTAB (Fig.5b) and PEG (Fig.5c) assisted samples.

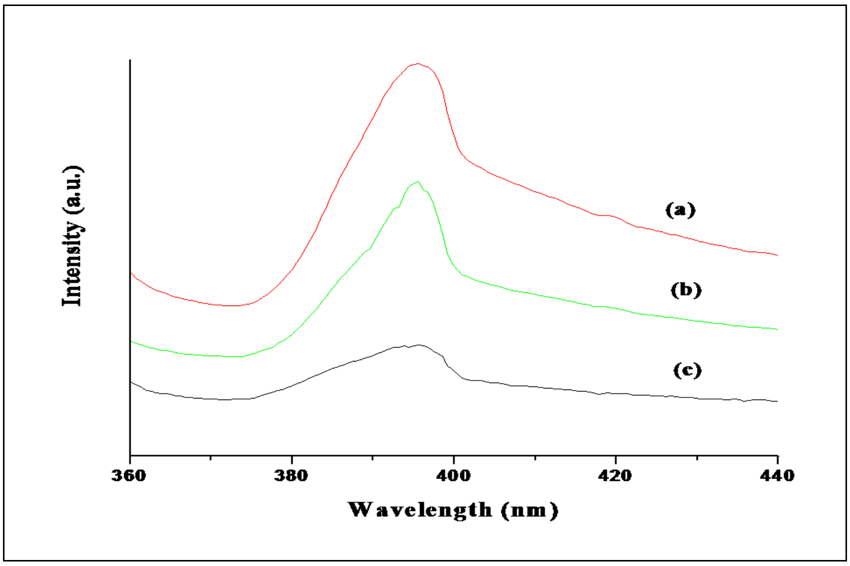

Fig.5. Photoluminescence spectra of tin oxide nanoparticles (a) PEG, (b) CTAB, and (c) SDS.

The emission in the UV region is called the near band-edge emission, generated by the free-exciton recombination and the visible region known to be deep-level emission appearing because of the impurities and structural defects in the structures. The UV emission is originated from excitonic recombination corresponding to the near-band-edge emission of SnO_2. However, the absence of green-yellow and orange-red emissions in the sample indicates the potential to produce a low concentration of oxygen defects and high optical quality of crystalline SnO_2. All the spectra in this study showed high UV emission and very low blue-green emission. The high UV to visible emission ratio indicates a good crystal quality of the nanoparticles, i.e. a low density of surface defects.

4. Conclusions

Hydrothermal synthesis of nanocrystalline SnO_2 powders of about 8-13nm in size have been successfully synthesized by using different surfactants such as CTAB, SDS, and PEG. On the other hand, the morphologies of the as-synthesis SnO_2 nanocrystallites are dependent on the surfactant. The addition of surfactant can influence particle growth, coagulation, and flocculation. Therefore, surfactants play an important role in the preparation of metal oxide nanoparticles. Moreover, the SnO_2 nanoparticles have a very strong PL band at ultraviolet wavelength range. The as-synthesized SnO_2 nanoparticles are promising materials for nanoscale optoelectronic devices due to their excellent UV emission properties.

Acknowledgement

The authors are grateful to the University Grant Commission for extending financial support to carry out this work.

References

[1] D. S. Kumar, P. R. Carbarrocas, J. M. Siefert, Appl. Phys Lett. **54,** 2088 (1989).
[2] A. Lousa, S. Gimeno, J. Marti, Vacumm **45,** 1143 (1994).
[3] A. Tsunashima, H. Yoshimizu, K. Kodaira, S. Shimada, T. Matsushits, J. Mater. Sci. **21**, 2731 (1986).
[4] S. Ferrere, A. Zaban, B. A. Gregg, J. Phys. chem. B **101,** 4490 (1997).
[5] Y. Tachibana, K. Hara, S. Takano, K. Sayama, H. Arkawa, Chem. Phys. Lett. **364,** 297 (2002).
[6] D. Wang, S. Wen, J. Chen, S. Zhang, F. Li, Phys. Rev. B **49,** 14282 (1994).
[7] Z. W. Chen, J. K. L. Lai, C. H. Shek, Phys. Rev. B **70,** 165314 (2004).
[8] A. Dieguez, A. R. Rodriguez, A. Vila, J. R. Morante, J. Appl. Phys. **90,** 1550 (2001).
[9] T. Arai, J. Phys. Soc. Jpn. **15,** 916 **(**1960).
[10] J. Jeong, S. P. Choi, C. I. Chang, D. C. Shin, J. S. Park, B. T. Lee, Y. J. Park, H. J. Song, Solid State Commun.**127,** 595 (2003).
[11] L. R. B. Santos, T. Chartier, C. Pagnoux, J. F. Baumard, C. V. Santilli, S. H. Pulcinelli, A. Larbot, J. Eur. Ceram, Soc. **24,** 3713 (2004).
[12] B. Grzeta, E. Tkalcec, C. Goebbert, M. Takeda, M. Takahashi, K. Nomura, M. Jaksic, J. Phys. Chem. Solids **63,** 765 (2002).
[13] J. A. T. Antonio, R. G. Baez, P. J. Sebastian, A. Vazquez, J. Solid state Chem.**174,** 241 (2003).
[14] J. Zhang, L. Gao, J. Solid State Chem. **177,** 1425 (2004).
[15] D. U. Lee, S. R. Jang, R. Vittal, J. Lee, K. J. Kim, Solar ener. **82,** 1042 (2008).
[16] C. Y. Hu, S. L. Lo, C. M. Li, W. H. Kuan, J. Hazardous. Mat.A. **120,** 15 (2005).
[17] Raghumani Singh Ningthoujam, S. K. Kulshreshtha, J. Mat. Res. Bullet. **6,** 4147 (2008).